RESILIENT INFRASTRUCTURE
June 1–4, 2016
RESILIENT INFRASTRUCTURE LONDON 2016

EFFECT OF SHEAR SPAN TO DEPTH RATIO ON SEISMIC PERFORMANCE OF REINFORCED MASONRY SHEAR WALLS

Hany M. Seif ElDin
PhD Candidate, Concordia University, Canada

Khaled Galal
Professor, Concordia University, Canada

ABSTRACT

Over the past few decades there has been a substantial increase in the number of multi-story buildings constructed with reinforced masonry (RM). Similar to reinforced concrete (RC) buildings, shear walls are a popular lateral load resisting system in regions of high seismic activity due to its capability to provide lateral stiffness, strength and energy dissipation. One of the parameters that affects the inelastic behaviour and ductility of RM shear walls is the shear span to depth ratio, M/Vd_v. This paper experimentally investigates the effect of M/Vd_v on the seismic performance of RM shear walls that are dominated by diagonal shear failure. The experimental work involves two identical full-scale fully grouted rectangular RM shear walls, W-M/Vd_v1.2 and W-M/Vd_v1.8, tested under in-plane axial compressive stress and cyclic lateral excitations. Wall W-M/Vd_v1.8 was subjected to a top moment so that M/Vd_v was equal to 1.875, as compared to a value of 1.25 for wall W-M/Vd_v1.2 that was tested without a top moment. Most of the existing design equations for nominal in-plane shear strength, V_n, for RM shear walls, including the current provisions of the Canadian Standards CSA S304-14, the Masonry Standards Joint Committee MSJC (2013), and the New Zealand code (2004) for masonry structures, limit the effect of the M/Vd_v to an upper value of 1.0. The test results show a significant reduction of 25% in the shear strength when M/Vd_v is increased, which means that limiting the effect of M/Vd_v to an upper value of 1.0 is overestimating the V_n of RM shear walls at high values of M/Vd_v. However, W-M/Vd_v1.8 was able to achieve higher levels of displacement ductility. More results were analyzed and are presented in this paper according to force-based, displacement-based, and performance-based seismic design considerations.

Keywords: Reinforced masonry; Shear walls; Seismic performance; Shear span to depth ratio.

1. INTRODUCTION

Masonry structural walls are key structural elements commonly used to resist lateral loads in masonry buildings. Post-earthquake reconnaissance and experimental research work (Sveinsson et al., 1985; Matsumura, 1986; Shing et al., 1990) have shown that there are several failure modes for masonry shear walls such as:

1. Flexural failure (including flexural cracks, yielding of longitudinal reinforcement, and crushing of masonry);
2. Shear failure (diagonal tension cracking, yielding of transversal reinforcement, and sliding); and
3. Flexural/shear failure.

The shear span to depth ratio, M/Vd_v, is one of the parameters that have a considerable effect on the inelastic behaviour of RM shear walls and the demand level of ductility. Furthermore, it is a good numerical indicator for the interaction between flexural behaviour and shear behaviour. Anderson and Priestley (1992) proposed the first effective equation that considered V_n as the sum of three independent terms provided by: masonry, V_m, axial compression load, V_p, and horizontal reinforcement, V_s. However, the equation proposed by Anderson and Priestley (1992) did not consider the effect of the shear span to depth ratio, M/Vd_v, or the wall aspect ratio, h_w/l_w, on V_n. They explained that all the walls in their data sets for calibrating their proposed equation had a height to width ratio, h_w/l_w, greater than 1.0 with most of them ranging between 1.0 and 1.6. The walls tested by Shing et al. (1990) had single

curvature bending with h_w/l_w equal to 1.0, while tests by Sveinssion et al. (1985) and Matsumura (1986) had double curvature bending with equal top and bottom moments, where M/Vd_v was less than one for most of their tested walls. Since their proposed equation did not appear to fit one set of data better than the other, they concluded that the in-plane shear behaviour of RM shear walls with h_w/l_w greater than unity is not affected by the wall aspect ratio.

On the other hand, most of the existing design equations for the nominal in-plane shear strength, V_n, for RM shear walls, including the current provisions of the Canadian Standards CSA S304-14, the Masonry Standards Joint Committee MSJC (2013), and the New Zealand code (2004) for masonry structures, consider a reduction in the masonry contribution, V_m, by increasing M/Vd_v. However, M/Vd_v is limited to an upper value of 1.0. This upper limit could be explained by all of the proposed equations having been developed based on the results of experimental work. The majority of the tested RM walls from this experimental data had a shear span to depth ratio, M/Vd_v, less than 1.5 due to the limitations in the height of the testing machine. To investigate the behaviour of shear walls with higher values of M/Vd_v, recent research was conducted on half scale concrete blocks (Banting and El-Dakhakhni, 2012) or by applying a top moment on RC shear walls (El-Sokkary and Galal, 2013) as used in this paper. More discussion about the different equations for V_n, including the design equations given in CSA S304-14 and MSJC-2013, is presented in Seif ElDin and Galal (2015).

2. EXPERIMENTAL PROGRAM

To study the effect of the shear span to depth ratio, M/Vd_v, on the seismic performance of RM shear walls, two identical RM walls W-M/Vd_v1.2 and W-M/Vd_v1.8 were tested without and with a top moment respectively. Both walls had the same dimensions of 1.8 m x 1.6 m x 0.19 m and were subjected to a cyclic lateral load at a height of 1.8 m from the base RC footing to have a minimum height-to-length ratio, h_w/l_w, equal to 1.0. Most of the masonry design codes classify shear walls based on h_w/l_w. The Canadian Standards CSA S304-14 provide special provisions for seismic design of low-aspect-ratio (squat) shear walls with h_w/l_w less than 1.0. Wall W-M/Vd_v1.8 was subjected to a top moment of 0.9V kN.m, where V is the lateral load from the horizontal actuator, which makes the shear span to depth ratio, M/Vd_v, and the overall height-to-length ratio, h_w/l_w, equal to 1.875, 1.5 as compared to values of 1.25, 1.0 for wall W-M/Vd_v1.2, respectively. The two walls were vertically reinforced with 20M bar in each cell with a vertical reinforcement ratio, ρ_v, of 0.79%, in addition to uniformly vertical distributed horizontal reinforcement of 10M@400 mm c/c, ρ_h = 0.13%. The horizontal reinforcement bars were hooked using a standard 180° bend around the outermost wall flexural reinforcing bars. A constant axial compressive stress of 1.0 MPa was applied to the studied walls before subjecting them to in-plane cyclic lateral displacements and it remained constant during the whole test. Table 1 summarizes the design details of the tested walls. The tested walls and the required auxiliary specimens were constructed in the structures laboratory at Concordia University with the help of certified masons following all the requirements of the Canadian Standards CSA S304-14 and CSA A179-14.

Table 1: Full-scale masonry walls design details

Wall ID	Wall dimensions			Reinforcement		Axial stress	Applied top	M/Vd_v **
	Height h_w	Length l_w	Width b_w	Vertical	Horizontal	σ_n	Moment	
	mm	mm	mm	---	---	MPa	kN.m	---
W-M/Vd_v1.2	1600	1800	190	20M@200	10M@400	1.0	0.0	1.25
W-M/Vd_v1.8	1600	1800	190	20M@200	10M@400	1.0	0.9V*	1.875

* V = the lateral load from the horizontal actuator

** $d_v = 0.8l_w$ (as defined in CSA S304-14)

Three MTS hydraulic actuators were used to apply the loads as shown in Figure 1. Two actuators were installed vertically and were used to apply the axial compressive stress, in addition to the top moment on the top of wall W-M/Vd_v1.8. The in-plane cyclic excitations were applied using the horizontal actuator. The applied lateral displacement was measured as the difference between the average readings of the top displacements from both directions of loading. To define the yield displacement, four strain gauges were installed at the wall-footing interface of the two outermost vertical reinforcement bars on each side. For adequate monitoring of the axial strain distribution along the transverse reinforcement, five 5mm strain gauges were distributed equally along the total length of each bar. Using the experimentally measured stress-strain curve and cross-section area for the steel reinforcing bars, the transverse reinforcement contribution, V_s, to the in-plane shear strength, V_n, was calculated. The

loads were applied in two phases. In the first phase, the total vertical compression load was applied using load-control protocol. The test protocol was switched to displacement-control in the second phase, by introducing in-plane lateral displacements at the middle height of the loading steel beam, following the loading histories proposed by FEMA 461 (2007). In each stage of lateral loading, two displacement cycles were completed for each target displacement increment. More details about the material properties, test setup, instrumentations, and test protocol can be found in Seif ElDin and Galal (2015).

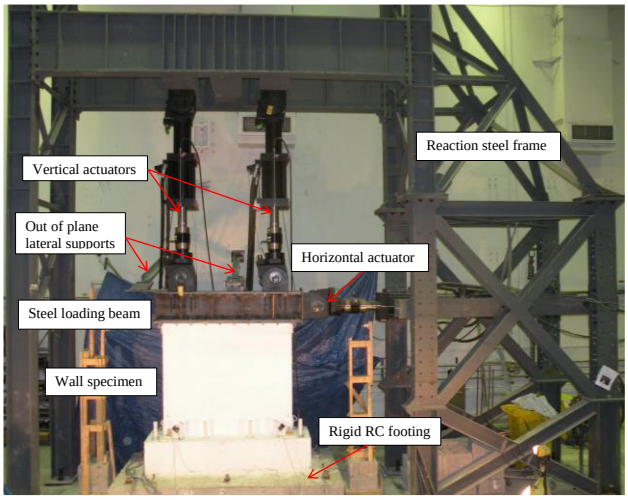

Figure 1: Test setup

3. EXPERIMENTAL RESULTS

The two tested walls exhibited shear dominated response with diagonal cracks as shown in Figure 2. The hysteretic force-displacement response for each wall against the top drift is given in Figure 3, furthermore, Table 2 summarizes the test results including the crack, yield, and ultimate capacities in addition to the drift limit of 1%. In this table, the lateral yield displacement, Δ_y, is taken as the average between the top lateral displacements corresponding to the first yield in the vertical reinforcement in each direction, Q_{ue} is the lateral peak load, $\Delta_{0.8Que}$ is the top lateral displacement defined at a drop in wall capacity to 80% of Q_{ue}, and $\mu_{\Delta e1\%}$ is the lateral displacements ductility corresponding to the top drift of 1.0%. As shown in Figure 3 and Table 2, both tested walls had a similar behaviour in both push and pull directions with a general symmetric resistance. Thus, only the results in the push direction were considered for the evaluation of the M/Vd_v on their seismic performance in terms of force-based, displacement-based, and performance-based seismic design considerations.

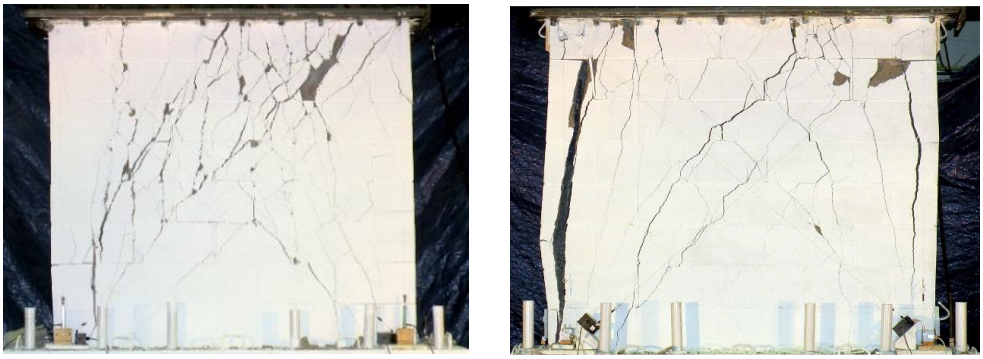

(a) W-M/Vd_v1.2 (b) W-M/Vd_v1.8

Figure 2: Crack pattern of tested walls at failure

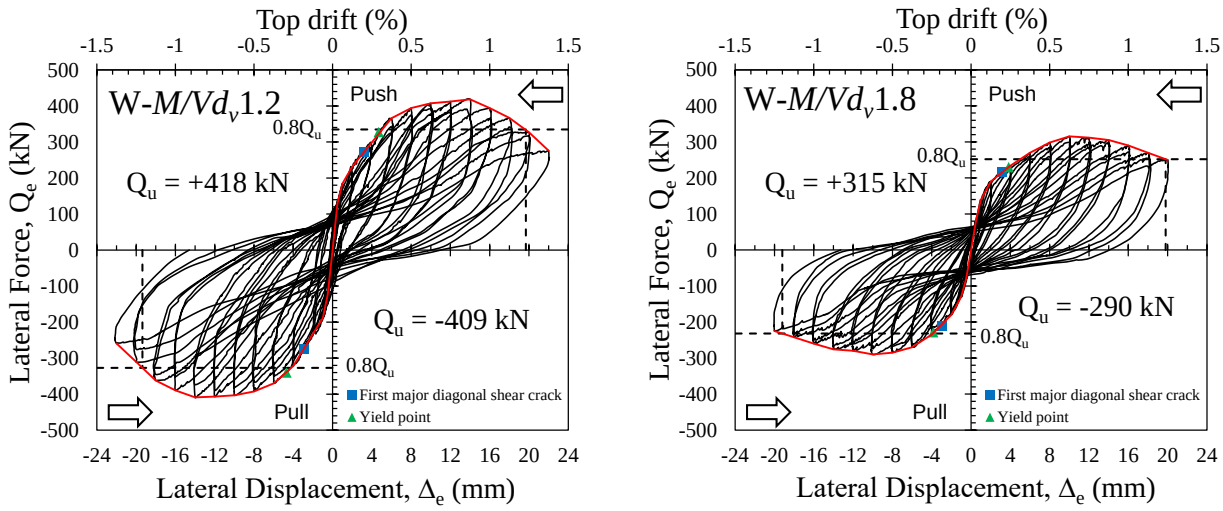

(a) W-M/Vd_v1.2 (b) W-M/Vd_v1.8

Figure 3: Lateral load-displacement hysteretic relationships and the backbone envelopes of tested RM shear walls

Table 2: Summary of test results

Wall ID	Test Results									
	Yield		Peak		Failure	Displacement ductility			First crack*	
	Q_{ye} (kN)	Δ_{ye} (mm)	Q_{ue} (kN)	Δ_{Que} (mm)	$\Delta_{0.8Que}$ (mm)	$\mu_{\Delta Que}$ ——	$\mu_{\Delta 0.8Que}$ ——	$\mu_{\Delta e1\%}$ ——	Δ_{FCe} (mm)	Q_{FCe} (kN)
W-M/Vd_v1.2	328	4.7	418	14.0	19.7	3.0	4.2	3.4	3.2	272
	-339	-4.7	-409	-14.0	-19.4	3.0	4.1	3.4	-2.9	-274
W-M/Vd_v1.8	230	3.8	315	10.0	19.8	2.6	5.2	4.2	3.2	216
	-225	-3.7	-290	-10.0	-19.2	2.7	5.3	4.4	-3.0	-210

* First major diagonal crack

3.1 Force-Based Design

Force-Based Design (FBD) is one of the current approaches for seismic design, which is widely used in many modern seismic codes including the National Building Code of Canada (NBCC 2010). In this approach, the behaviour of structures is simulated by a single-degree-of-freedom (SDOF) system. As such, the design seismic base shear is obtained from the estimated equivalent fundamental mode period and the mass of structure participating in the first mode. The design force from this approach is mostly limited by a certain level of deformation in terms of ductility or inter-story drifts. Most of the existing equations for the nominal in-plane shear strength of RM shear walls, V_n, consider it as the sum of three independent terms provided by: masonry, V_m, axial compressive stress, V_p, and horizontal reinforcement, V_s. The measured strain readings along the horizontal reinforcement were used to calculate V_s. Next, the sum of the contributions from the masonry and axial compressive stress V_{m+p} was calculated as the difference between V_n and V_s.

The test results presented in Figure 4 show a reduction in the achieved ultimate force, Q_{ue}, of 25% due to increasing M/Vd_v from 1.25 to 1.875. This loss in the shear resistance is accompanied by enhancement in the displacement ductility, $\mu_{\Delta 0.8Qu}$, from 4.2 to 5.2. However, the crack strength of wall W-M/Vd_v1.8 was 30% less than wall W-M/Vd_v1.2. Also, it can be noticed that Wall W-M/Vd_v1.8 achieved its yield capacity at a lateral load, Q_{ye}, of 230 kN compared to 328 kN when the same wall was tested without a top moment.

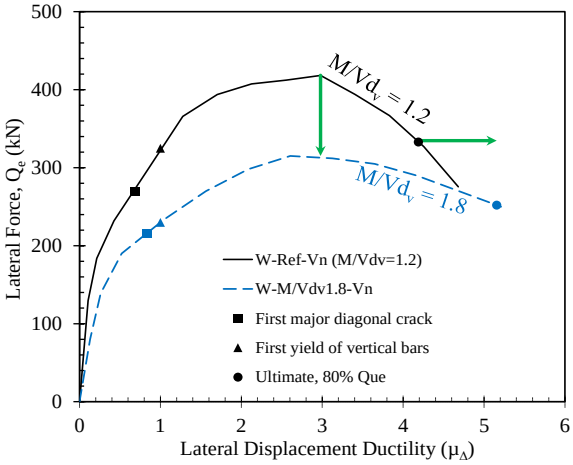

Figure 4: Effect of shear span to depth ratio, M/Vd_v, on in-plane shear strength of RM shear walls

Figure 5 illustrates the effect of M/Vd_v on shear resistance shares provided by horizontal reinforcement, V_s, and masonry and axial compressive stress, V_{m+p}. The shear span to depth ratio did not show a significant effect on V_s since the horizontal reinforcement in both walls reached its yield capacity at the same μ_Δ of 3.0. At an early stage of ductility, the shear resistance provided by V_s in wall W-M/Vd_v1.8 was higher than W-M/Vd_v1.2 because wall W-M/Vd_v1.8 reached its inelastic deformations earlier. On the other hand, the aforementioned reduction in Q_{ue} due to increasing M/Vd_v from 1.25 to 1.875, could be due to losses in $(V_{m+p})_{max}$ as shown in Figure 5b. In wall W-M/Vd_v1.2, the masonry and axial compressive stress contributed with an ultimate resistance of 275 kN at μ_Δ of 1.27 followed by rapid strength degradation. This behaviour became more ductile in wall W-M/Vd_v1.8 with less capacity, $(V_{m+p})_{max}$, equal to 155 kN.

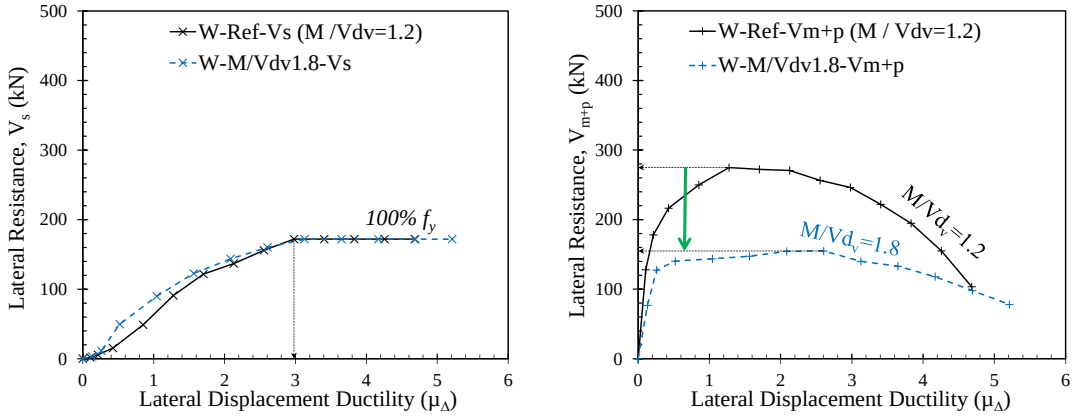

Figure 5: Effect of shear span to depth ratio, M/Vd_v, on shear resistance shares provided by: (a) horizontal reinforcement, V_s; (b) masonry and axial compressive stress, V_{m+p}

The test results presented here show that limiting the effect of shear span to depth ratio, M/Vd_v, to an upper value of 1.0, as provided in most of the masonry design codes including the Canadian Standards Association CSA S304-14, the US Masonry Standards Joint Committee MSJC-2013, and the Standards Association of New Zealand NZS 4230:2004, is overestimating V_n at high values of M/Vd_v, which might lead to an unsafe design. This experimentally measured reduction in the shear capacity could be explained by considering the interaction between the flexural and shear performances, as shown in Figure 6. Both walls are identical in dimensions and reinforcement such that they have the same shear strength envelope and moment capacity. Increasing M/Vd_v results in a reduction in the lateral force that corresponds to the flexural capacity of the wall. Consequently, this lower lateral force intersects with the shear strength envelope at a lower capacity along with higher displacement ductility.

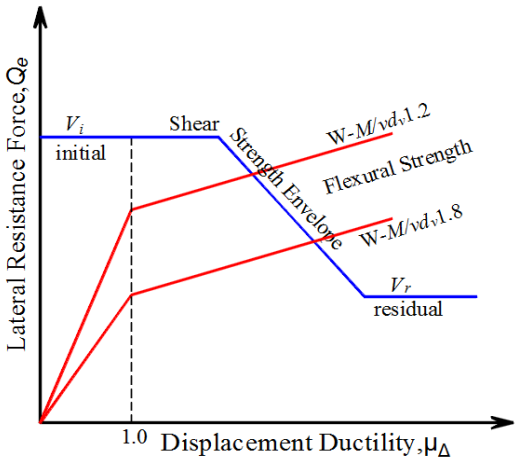

Figure 6: Interaction between flexural and shear performance of tested walls

3.2 Displacement-Based Design

Unlike the force-based design that intends to keep the inter-story drifts to less than a certain limit when the structure is subjected to the design seismic force, the displacement-based design approach aims to achieve a target level of building performance under a specified level of seismic intensity in terms of demand top drift or lateral displacement, Δ_d. Stiffness degradation, energy dissipation, and equivalent viscous damping are important aspects that need to be considered when evaluating the seismic performance of RM shear walls, as well as when modeling their cyclic response. In this paper, these three parameters are calculated for each tested wall at different levels of top drift and are taken into account when evaluating the effect of shear span to depth ratio, M/Vd_v.

3.2.1 Stiffness Degradation

The acting lateral force on structures could be distributed among the shear walls based on their lateral stiffness. Thus, it is important to predict the degradation in the stiffness at the ultimate limit stage. In addition, stiffness degradation could be a good index for the level of damage in RM shear walls. The secant stiffness at any loading cycle, $K_{s,i}$, was defined as the ratio between the lateral resistance, Q_i, and the corresponding top lateral displacement, Δ_i. The initial gross stiffness, K_g, was calculated at the first cycle of ± 0.5 mm. Therefore, the secant stiffness degradation can be calculated as follows:

$$[1] \quad Stifness\,Degradation\,(\%) = \frac{K_{s,i}}{K_g} \times 100$$

The influence of M/Vd_v on the secant stiffness and the stiffness degradation is presented in Figure 7. Increasing M/Vd_v reduces the initial gross stiffness, K_g, since wall W-M/Vd_v1.8 had K_g equal to 160 kN/mm compared to 259 kN/mm for wall W-M/Vd_v1.2. However, the difference in the secant stiffness at the same level of top drift became smaller as the tested walls reached higher levels of deformation (see Figure 7a). Both walls reached their peak lateral load at the same secant stiffness of 30 kN/;mm. Nevertheless, wall W-M/Vd_v1.2 achieved its maximum resistance at a higher top drift of 0.875% compared to 0.625% for wall M/Vd_v1.8. On the other hand, increasing M/Vd_v enhanced the stiffness degradation as shown in Figure 7b. Wall W-M/Vd_v1.8 had about 50% reduction in its initial stiffness at a top drift of 0.18%, while wall W-M/Vd_v1.2 had the same stiffness degradation at earlier levels of deformation with a top drift of 0.11%. At a drift limit of 1%, the values of K_{sc} were 9.5% and 11.3% of the corresponding K_g when M/Vd_v was equal to 1.25 and 1.875, respectively. Moreover, as shown in Figure 7c, wall W-M/Vd_v1.8 had a gradual degradation in its secant stiffness related to the secant stiffness at the peak load, K_{sc}/K_{Que}, during the post-peak behaviour compared to wall W-M/Vd_v1.2.

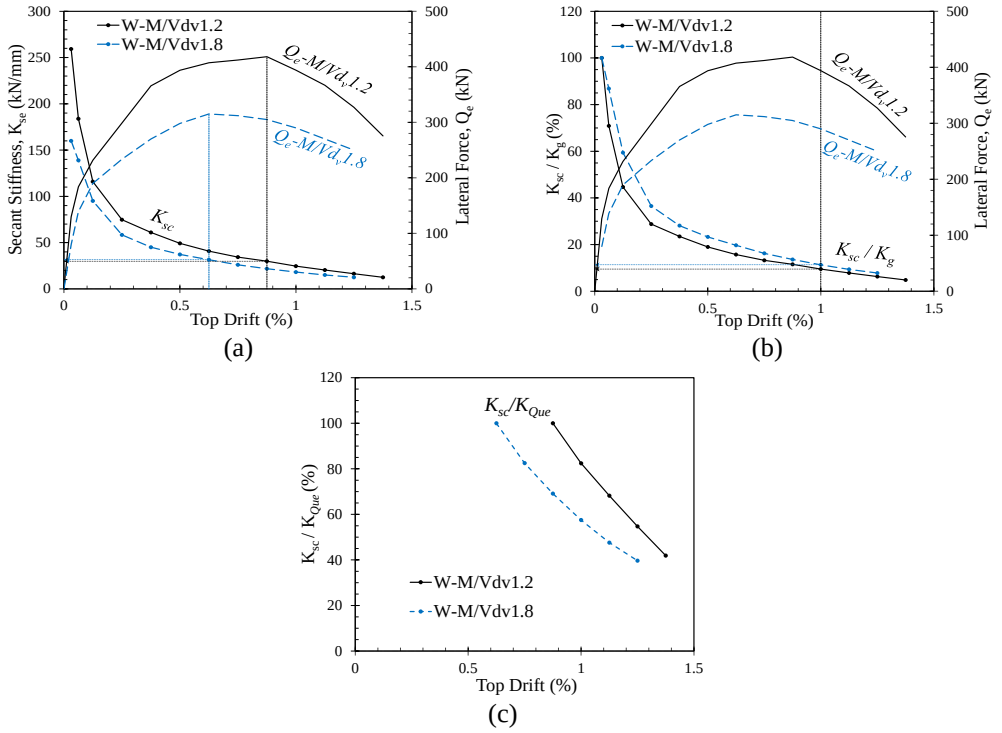

Figure 7: Effect of shear span to depth ratio, M/Vd_v, on stiffness degradation: (a) K_{sc}; (b) K_{sc}/K_g; (c) K_{sc}/K_{Que}

3.2.2 Energy Dissipation and Equivalent Viscous Damping Ratio

The capacity of shear walls to dissipate energy is another important aspect in seismic design and in analysis of their cyclic response. The energy dissipation, E_d, was defined as the area enclosed within the inelastic hysteretic force-displacement response, as proposed by Hose and Seible (1999). However, the elastic stored strain energy, E_s, was calculated as the area under the equivalent linear elastic response. The energy dissipation within different structure systems at the inelastic behaviour can be quantified through hysteric damping. Chopra (2000) described the hysteric damping by an equivalent viscous damping ratio, ζ_{eq}, using an equal area approach by equating the energy dissipated by a viscous damper with the energy dissipated from non-linear behaviour using the following equation:

$$[2] \quad \zeta_{eq} = \frac{1}{4\pi}\frac{E_d}{E_s}$$

Damping is generally specified for the whole structure rather than for an individual element. However, most RM structures are typically constructed with RM shear walls that are connected together by rigid diaphragms. Consequently, the trend of damping for a structural element such as shear walls, with respect to the top drift or the displacement ductility, can provide an indication for the overall response of RM structures. Figure 8 presents the total energy dissipation, E_d, and the equivalent viscous damping ratio, ζ_{eq}, of the tested walls at different levels of top drift. Since both walls were subjected to the same cyclic in-plane lateral displacement up to a top displacement of 20.0 mm and top drift of 1.25%, comparison between total energy dissipation can be conducted at same top drift. At a top drift limit of 1%, wall W-M/Vd_v1.2 dissipated 30% higher total energy than wall W-M/Vd_v1.8. This percentage decreased to 26% when both walls had a drop in their in-plane lateral force capacity to 80% of Q_{ue}, since wall W-M/Vd_v1.2 was able to dissipate total energy of 36.1 kN.mm compared to 28.5 kN.mm for wall W-M/Vd_v1.8. As can be noticed from the same figure, the shear span to depth ratio did not show a significant impact on the equivalent viscous damping ratio, ζ_{eq}. W-M/Vd_v1.2 had a ζ_{eq} that ranged between 9% and 17% with an average of 14% (c.o.v. = 15%). This range is slightly narrower for wall W-M/Vd_v1.8, which varied between 12% and 18% with an average of 14.4% (c.o.v. = 13%). However, after a top drift of 0.25% and up to failure, both walls had an average ζ_{eq} of 14.4% (c.o.v. = 9.1%).

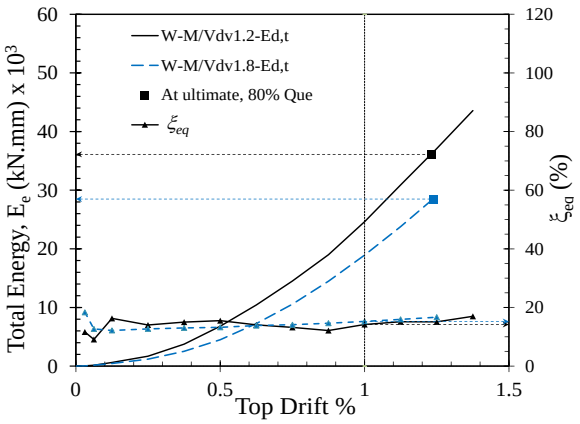

Figure 8: Effect of M/Vd_v on energy dissipation and equivalent viscous damping ratio, ζ_{eq}

3.3 Performance-Based Design

Both walls W-M/Vd_v1.2 and wall W-M/Vd_v1.8 had similar crack propagation and were characterized by moderately ductile failure as shown in Figure 9. Initial diagonal crack damage was observed at a top drift of 0.2% for both walls. As the imposed in-plane top lateral displacement increased, more cracks were formed and gradually spread over the wall diagonals. Wall W-M/Vd_v1.8 reached its lateral load capacity at early levels of deformation when subjected to top displacement of +10.0 mm; instead, Wall W-M/Vd_v1.2 was able to gain more resistance until Δ_e was equal to +14.0 mm. Yet, wall W-M/Vd_v1.8 required more loading cycles to lose 20% of its shear strength, Q_{ue}, compared to Wall W-M/Vd_v1.2. The two tested walls reached their failure point at almost the same Δ_e with an average top drift of 1.23%. However, increasing M/Vd_v from 1.25 to 1.875 resulted in higher levels of axial compressive stress on the end zones. Hence, buckling failure was observed in W-M/Vd_v1.8 as shown in Figure 9c. Nevertheless, this failure occurred in the wall cover outside the confined core as presented in Figure 10. As shown in this figure, the right side view of the final crack pattern for wall W-M/Vd_v1.8 does not show any inside crushing in the grout, which could explain the enhancement in the stiffness degradation during the post-peak behaviour.

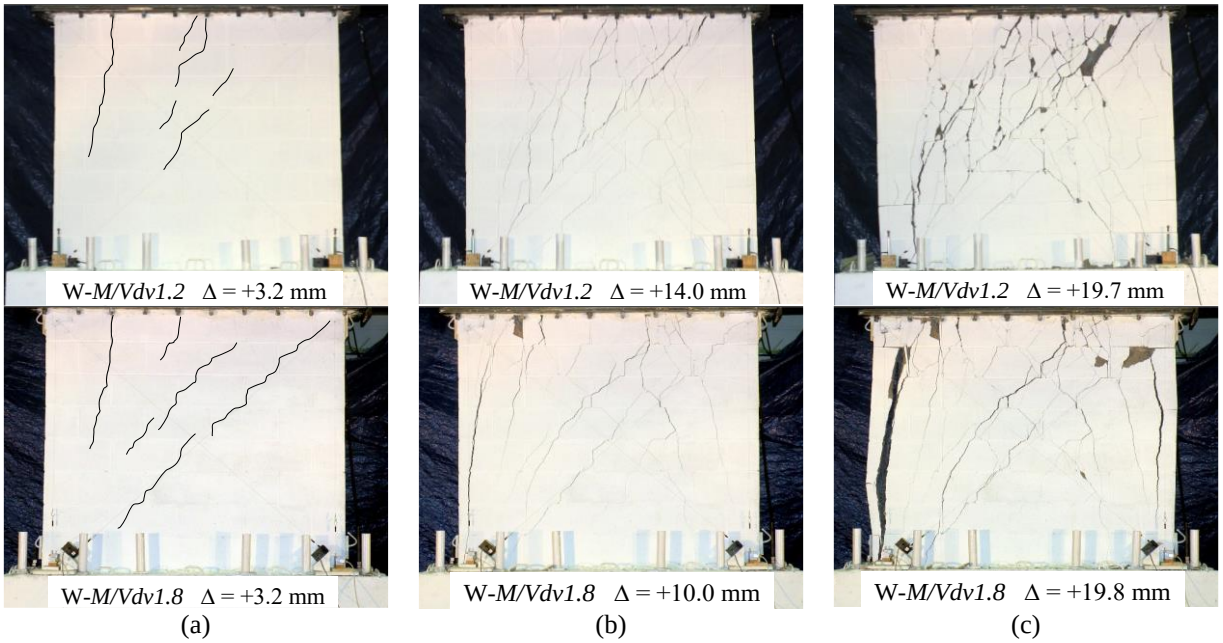

(a) (b) (c)

Figure 9: Effect of shear span to depth ratio, M/Vd_v, on crack pattern at: (a) first major diagonal cracks; (b) lateral peak load Q_{ue}; (c) when the lateral load dropped to 80% of Q_{ue}

W-*M/Vdv1.8* at the end of testing

Right side view

Figure 10: Final crack pattern of tested wall W-M/Vd_v1.8

4. SUMMARY AND CONCLUSIONS

One of the parameters that have a considerable effect on seismic performance of RM shear walls is the shear span to depth ratio, M/Vd_v. This paper involved assessing experimentally the in-plane shear behaviour of two single-story RM shear walls when subjected to in-plane axial compressive stress and cyclic lateral excitations. Two identical fully grouted RM walls, W-M/Vd_v1.2 and W-M/Vd_v1.8, were tested without and with a top moment to have M/Vd_v equal to 1.25 and 1.875, respectively.

The test results show a significant reduction in the shear strength by 25% when M/Vd_v is increased. These results clarify that limiting the effect of M/Vd_v to an upper value of 1.0, as provided in most of the masonry design codes, is overestimating V_n of RM shear walls at high values of M/Vd_v, which might lead to an unsafe design. However, increasing M/Vd_v enhanced the stiffness degradation and was accompanied by more ductile behaviour. W-M/Vd_v1.8 was able to achieve higher displacement ductility, $\mu_{\Delta 0.8Que}$, of 5.2 compared to 4.2 for wall W-M/Vd_v1.2. This behaviour could be explained by considering the interaction between the flexural and shear performances. Both walls were identical in dimensions and reinforcement such that they have the same shear strength envelope and moment capacity. Increasing M/Vd_v results in a reduction in the lateral force that corresponds to the flexural capacity of the wall. Consequently, this lower lateral force intersects with the shear strength envelope at a lower capacity along with higher displacement ductility. On the other hand, the tested wall without a top moment, M/Vd_v equal to 1.25, dissipated 30% higher total energy than the tested wall with a top moment, M/Vd_v, equal to 1.875. It was also noticed that the shear span to depth ratio, M/Vd_v, has a slight influence on the equivalent viscous damping ratio, ζ_{eq}.

ACKNOWLEDGEMENTS

The authors would like to acknowledge the support of the Natural Science and Engineering Research Council of Canada (NSERC). This work was conducted in collaboration with the Canada Masonry Design Centre (CMDC) and the Canadian Concrete Masonry Producers Association (CCMPA).

REFERENCES

Anderson, D. L., and Priestley, M. J. N. 1992. In Plane Shear Strength of Masonry Walls. *6th Canadian Masonry Symposium*, Saskatoon, Canada: 223-234.

Banting, B. and El-Dakhakhni, W. 2012. Force- and Displacement-Based Seismic Performance Parameters for Reinforced Masonry Structural Walls with Boundary Elements. *J. Struct. Eng.*, ASCE, 138(12): 1477–1491.

Chopra, A. K. 2007. *Dynamics of Structures: Theory and Applications to Earthquake Engineering*. Third Edition, Pearson Prentice Hall, Upper Saddle River, New Jersey, USA.

CSA S304-14. 2014. *Design of Masonry Structures*. Canadian Standards Association (CSA), Mississauga, Canada.

CSA A179-14. 2014. *Mortar and Grout for Unit Masonry*. Canadian Standards Association (CSA), Mississauga, Canada.

El-Sokkary, H., and Galal, K. 2013. Seismic Behaviour of FRP-Strengthened RC Shear Walls. *J. Composites for Construction*, ASCE, 17(5): 603–613.

FEMA 461. 2007. *Interim Testing Protocols for Determining the Seismic Performance Characteristics of Structural and Nonstructural Components*. Federal Emergency Management Agency (FEMA), Report No. 461, Washington, USA.

Hose, Y. D., and Seible, F. 1999. Performance Evaluation Database for Concrete Bridge Components and Systems under Simulated Seismic Loads. *Pacific Earthquake Engineering Research Center* (PEER), Report No. 1999/11, College of Engineering, University of California, Berkley, USA.

Matsumura, A. 1986. Shear Strength of Reinforced Hollow Unit Masonry Walls. *2nd Meeting of the U.S.-Japan Joint Technical Coordinating Committee on Masonry Research*, Keystone, USA.

MSJC. 2013. *Building Code Requirements for Masonry Structures*. Masonry Standards Joint Committee, TMS 402/ ACI 530/ASCE 5, The Masonry Society, American Concrete Institute, and American Society of Civil Engineers, Boulder, CO, Farmington Hills, MI, and Reston, VA, USA.

NBCC. 2010. *National Building Code of Canada*. National Research Council of Canada. Ottawa, Canada.

NZS 4230:2004. 2004. *Design of Reinforced Concrete Masonry Structures*. Standards Association of New Zealand (SANZ). , Wellington, New Zealand.

Seif ElDin, H. M., and Galal, K. 2015. Influence of Axial Compressive Stress on the In-Plane Shear Performance of Reinforced Masonry Shear Walls. *11th Canadian Conference on Earthquake Engineering*, Victoria, BC, Canada.

Seif ElDin, H. M., and Galal, K. 2015. Survey of Design Equations for the In-Plane Shear Capacity of Reinforced Masonry Shear Walls. *12th North American Masonry Conference*, Denver, Colorado.

Shing, P., Schuller, M., and Hoskere, V. 1990. In-Plane Resistance of Reinforced Masonry Shear Walls. *J. Struct. Eng.*, ASCE, 116(3): 619-640.

Sveinsson, B. I., Mayes, R. L., and McNiven, H. D. 1985. Cyclic Loading of Masonry single piers – Volume 4: Additional tests with height to width ratio of 1. Report No. UCB/EERC-85/15, *Earthquake Engineering Research Centre*, University of California, Berkeley. USA.